backward reactions are given in modified Arrhenius form. In contrast, the Park models were modified for thermodynamic nonequilibrium and are commonly referred to as "two-temperature" models. In this study, the Park models are used for thermodynamic equilibrium by assuming that the translational and vibrational temperatures are equivalent. The forward rate constants are again given by the Arrhenius equations. The backward rates, however, are obtained from a curve fit for the equilibrium constants using the well-known relation

$$k_b = \frac{k_f}{K_c} \tag{5}$$

Additionally, calculations were performed with a hybrid model that combines the Dunn and Kang forward rates with the backward rates obtained from Eq. (5) and the curve fits of Gupta et al.[9] for the equilibrium constants. Those fits were determined using 18 data points between 500 and 60,000 K and are more accurate than Park's fits at temperatures above 12,000 K.

Typical results of these comparisons are summarized in Figs. 3 and 4. In Fig. 3, the temperature distribution downstream from the normal shock wave is given as calculated by the four different models that include both of Parks,[6,8] the Dunn and Kang model, and the hybrid Dunn-Kang/Gupta mechanism. The largest discrepancy in the prediction of the relaxation zone occurs between the Park[6] and the Dunn and Kang models. The newer models, Park[8] and the hybrid model, tend to bridge the gap between the extreme predictions of the relaxation zone location. Note that there is very good agreement in the equilibrium value of the predicted temperatures

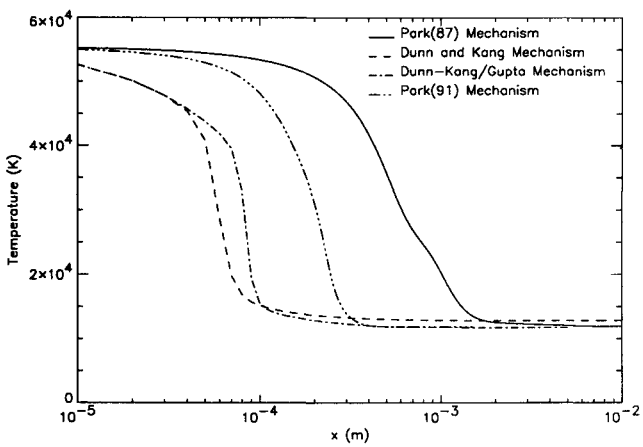

Fig. 3 Comparison of temperature distribution behind a $M = 33.70$, $h = 60.96$ normal shock wave for various kinetic models.

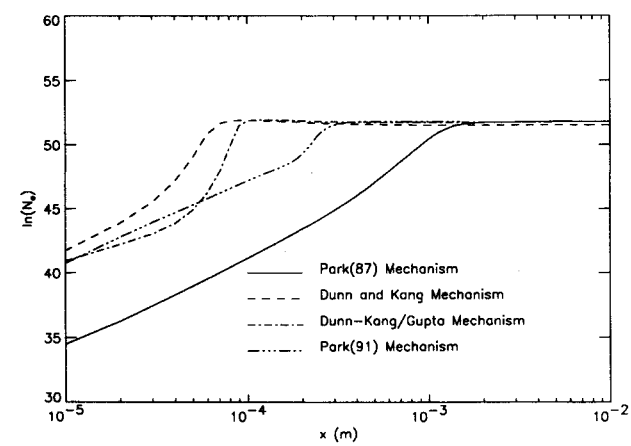

Fig. 4 Comparison of the electron number density behind a $M = 33.70$, $h = 60.96$ normal shock wave for various kinetic models.

downstream of the normal shock wave as predicted by the Park[8] and Dunn-Kang/Gupta mechanisms. This is probably the result of the improved curve fits for the equilibrium constants that were employed in these newer models. In Fig. 4, the logarithm of the electron number density is plotted vs distance downstream of the shock wave. Again, it is particularly evident that the Dunn and Kang model predicts the quickest reaction rate with the electron number density reaching a plateau more than one millimeter ahead of the location as predicted by Park.[6] As with the temperature profiles, the relaxation zones for the Park[8] and hybrid models are located between the two extremes. Thus the use of these newer models reduces the discrepancy in the flowfield predictions. However, the reader is cautioned that there may be some question as to the validity of the hybrid model. In particular, there is some current conjecture as to the validity of mixing and matching parts of reaction mechanisms. Finally, the purpose of the present work is to examine the discrepancy between various kinetic models; no conclusion can be made as to which model is the most correct without having some definitive experimental data with which to compare. Such data are lacking at present.

References

[1]Mitcheltree, R. A., "A Parametric Study of Dissociation and Ionization Models at 12 km/s" AIAA Paper 91-1368, June 1990.

[2]Weber, Y., and Anderson, J. D., Jr., "A Comparison of Chemical Kinetic Rate Mechanisms for High Temperature Air, Including Electronic Energy," Univ. of Maryland, UM-AERO-40, College Park, MD, 1991.

[3]Vincenti, W. G., and Kruger, C. H., *Introduction to Physical Gas Dynamics*, Wiley, New York, 1965, pp. 86–151.

[4]Anderson, J. D., Jr., *Hypersonic and High Temperature Gas Dynamics*, McGraw-Hill, New York, 1988, pp. 413–467.

[5]Dunn, M. G., and Kang, S. W., "Theoretical and Experimental Studies of Reentry Plasmas," NASA CR-2232, April 1973.

[6]Park, C., "Assessment of Two-Temperature Kinetic Model for Ionizing Air," AIAA Paper 87-1574, June 1987.

[7]Park, C., *Nonequilibrium Hypersonic Aerothermodynamics*, Wiley, New York, 1990.

[8]Park, C., "Chemical-Kinetic Problems of Future NASA Missions," AIAA Paper 91-0464, Jan. 1991.

[9]Gupta, R. N., Yos, J. M., Thompson, R. A., and Lee, K., "A Review of Reaction Rates and Thermodynamic and Transport Properties for an 11-Species Air Model for Chemical and Thermal Nonequilibrium Calculations to 30,000 K," NASA RP-1232, Aug. 1990.

Preferential Thermal and Multicomponent Species Transport Effects in Strained Diffusion Flames

J. C. Hermanson* and A. Vranos†
United Technologies Research Center, East Hartford, Connecticut 06108

Introduction

THE study of the structure of laminar diffusion flames is relevant to a number of combustion problems, such as flat flames established between opposing reactant jets and curved flames stabilized above porous spheres or cylinders.[1] In addition, laminar flame elements have been incorporated in

Received Sept. 16, 1991; revision received May 12, 1992; accepted for publication May 13, 1992.

*Research Scientist, Advanced Propulsion, Power, and Flight Systems, Mail Stop 29. Senior Member AIAA.

†Consulting Scientist, Environmental Sciences, Industrial Systems, and Technology, Mail Stop 30. Member AIAA.

the modeling of turbulent diffusion flames.[2] Diffusion flame structure is influenced strongly by the relative rates of the transport of molecular species and thermal energy. There have been numerous analytical studies of the effects of unequal *mass* transport on the properties of diffusion flames.[3-6] These analyses correspond physically to dilute reactants diffusing preferentially through a single inert; preferential *thermal* transport is not considered. It is not obvious that unequal thermal transport, either by itself or in combination with unequal mass transport, will have the same impact on flame characteristics as unequal mass transport alone, even when the reactant Lewis numbers are identical.

Some effects of preferential thermal transport in combination with preferential mass diffusion were examined by Hermanson and Vranos,[7] who took the thermal diffusivities to be unequal on different sides of the flame zone. In that case it was shown that the problem cannot be characterized in terms of reactant Lewis numbers alone. In the current study, the more physically realistic situation is considered whereby preferential thermal and mass transport effects arise from the interdiffusion of dissimilar species. The multicomponent diffusion model indicates a significant impact on flame temperature, flame front position, and reactant consumption rates as compared with models that consider mass transport due to binary diffusion only. Additional analysis and details not given in this Note are presented in Hermanson and Vranos.[8]

Analysis

The counterflow configuration is studied with the following principal assumptions: 1) fast chemistry, 2) constant strain rate, 3) no curvature, and 4) one-dimensional property variations. In addition, the reactants and products are taken to be sufficiently dilute so that mixture properties are a function of the temperature and inert species concentrations only. The two inerts are taken to have the same molecular weight but different specific heats and thermal conductivities. Although the previous assumptions do restrict the analysis, the results may illustrate fundamental effects of importance in more complicated systems.

The conservation equations for mass, species, and energy for the previous conditions are, respectively,

$$\epsilon\rho + \frac{\mathrm{d}}{\mathrm{d}y}(\rho v) = 0 \tag{1}$$

$$\rho v + \frac{\mathrm{d}\kappa_i}{\mathrm{d}y} + \frac{\mathrm{d}}{\mathrm{d}y} j_i = 0 \tag{2}$$

$$\frac{\mathrm{d}}{\mathrm{d}y}\left(\rho v H_{\mathrm{mix}} + \sum_i j_i H_i - k_{\mathrm{mix}} \frac{\mathrm{d}T}{\mathrm{d}y}\right) = 0 \tag{3}$$

where ϵ is the strain rate, ρ the total mass density, and v the velocity normal to the flame zone. The quantities $\kappa_i = \rho_i/\rho$ and j_i are, respectively, the mass fraction and diffusive mass flux of species i (say, $i = 1$ for the fuel, $i = 2$ for the oxidizer, and $i = 3$ and 4 for the inerts on the fuel and oxidizer side, respectively). The mass diffusion equation, Eq. (2), for $i = 1$ is valid for $y > y^+$; for $i = 2$ for $y < y^-$, where y^+ and y^- correspond to points immediately on the fuel or oxidizer side of the flame zone, respectively. The quantities H_{mix} and H_i are, respectively, the enthalpies of the mixture and for each species i; k_{mix} is the mixture thermal conductivity. The specific heat of each species is taken to be independent of temperature. The temperature boundary conditions are $T(y^+) = T(y^-) = T_F$, the flame temperature at the flame front, and $T(+\infty) = T(-\infty) = T_0$, the ambient temperature far from the flame zone. The corresponding boundary conditions on the reactant mass fractions are $\kappa_1(y^+) = \kappa_2(y^-) = 0$, $\kappa_1(+\infty) = \kappa_{01}$ and $\kappa_2(-\infty) = \kappa_{02}$. Similarly, the mass fractions of inert are taken to satisfy (for trace reactants) $\kappa_3(+\infty) = 1$, $\kappa_4(-\infty) = 0$ and $\kappa_4(-\infty) = 1$, $\kappa_3(-\infty) = 0$. Stoichiometric consumption of reactants and energy conservation at the flame front dictate, respectively,

$$j_1 = -f j_2 \tag{4}$$

$$-k_{\mathrm{mix}} \left.\frac{\mathrm{d}T}{\mathrm{d}y}\right|_{y^+} + k_{\mathrm{mix}} \left.\frac{\mathrm{d}T}{\mathrm{d}y}\right|_{y^-} = q j_1 \tag{5}$$

where f is the mass stoichiometric ratio of the reaction and q is the heat release of the chemical reaction per unit mass.

The diffusive mass flux of the inerts is given by the expression $j_i = -\rho D_{34}\, \mathrm{d}\kappa_i/\mathrm{d}y (i = 3, 4)$, where D_{34} is the binary diffusion coefficient of the inerts. For the reactants, the multicomponent diffusion flux implied by the interdiffusion of the inerts is written as $j_i = -\rho D_{im} \mathrm{d}\kappa_i/\mathrm{d}y (i = 1, 2)$ where D_{im} is the effective binary diffusivity in a multicomponent mixture, as given by Curtiss and Hirschfelder.[9] The mixture thermal conductivity is calculated using semi-empirical expressions developed by Mason and Saxena.[10]

The reactant mass diffusivities, mixture thermal conductivity, and total mass density are taken to be interrelated by the expression $\rho^2 D_{ij} = \rho^{*2} D_{ij}^*$ and $\rho k = \rho^* k^*$, where the asterisks denote isothermal local reference values. Thus, D_{im}^* and k^* are independent of temperature but vary with composition (i.e., position) owing to the interdiffusion of the inerts. The reference binary diffusivity of the inerts D_{34}^* and the local reference density ρ^* are constant. It is known that the approximations $\rho^2 D = \text{const}$ and $\rho k = \text{const}$ do suffer with increasing temperature. However, variations in $\rho^2 D$ and ρk tend to cancel each other out in the sense that, for fixed mixture composition, relatively little variation in reactant Lewis numbers is seen over a fairly wide temperature range. Furthermore, the earlier analysis of Hermanson and Vranos[7] suggests that the essential preferential thermal transport effects can be effectively characterized in terms of Lewis numbers and the ratio of transport properties (e.g., k_3^*/k_4^*), which can be nearly constant despite significant variations in the individual transport properties with temperature. The reactant Lewis numbers do change significantly with position owing to the variations in k^* and D_{im}^* brought about by the interdiffusion of the dissimilar inerts.

The scaling variable

$$\eta = \left[\frac{\epsilon}{2D_{34}^*}\right]^{1/2} \int_0^y \frac{\rho}{\rho^*}\, \mathrm{d}y$$

is introduced to allow for density variation owing to heat release. This choice of variable results in governing equations in which the local Lewis numbers based on the reactant diffusivities ($Le_i = \rho^* C_{p\mathrm{mix}} D_{im}^*/k_{\mathrm{mix}}^*$, $i = 1, 2$) do not appear explicitly. Solution of Eqs. (1) and (2) and enforcement of the boundary conditions give the following similarity solutions for reactant mass fraction:

$$\kappa_1 = \kappa_{01} \frac{F_1(\eta) - F_1(\hat{\eta})}{F_1(+\infty) - F_1(\hat{\eta})} \tag{6a}$$

$$\kappa_2 = \kappa_{02} \frac{F_2(\eta) - F_2(\hat{\eta})}{F_2(-\infty) - F_2(\hat{\eta})} \tag{6b}$$

where

$$F_i(\eta) \equiv \int_0^\eta \frac{D_{34}^*}{D_{im}^*} \exp\left(-2 \int_0^{\eta'} \eta'' \frac{D_{34}^*}{D_{im}^*}\, \mathrm{d}\eta''\right) \mathrm{d}\eta' \qquad i = 1, 2$$

and where $\hat{\eta}$ represents the location of the flame front. Equations (6a) and (6b) can be combined with the requirement of stoichiometric reactant consumption [Eq. (5)] to give an expression relating the flame front location to the equivalence ratio. The solutions for the temperature are obtained from the integration of Eq. (3):

$$T = \frac{G(\eta) - G(+\infty)}{G(\hat{\eta}) - G(+\infty)} \Delta T_F + T_0 \qquad \text{for} \qquad \eta > \hat{\eta} \tag{7a}$$

$$T = \frac{G(\eta) - G(-\infty)}{G(\hat{\eta}) - G(-\infty)} \Delta T_F + T_0 \qquad \text{for} \qquad \eta < \hat{\eta} \qquad (7b)$$

where

$$G(\eta) \equiv \int_0^{\eta} \frac{k_3}{k^*} \exp\left[- \int_0^{\eta'} Le_3 \left(\frac{k_3}{k^*}\right) \sum_{i=3,4} \left(2\kappa_i \eta'' + \frac{d\kappa_i}{d\eta''} \right) \frac{C_{p_i}}{C_p^*} \, d\eta'' \right] d\eta'$$

The Lewis number $Le_3 = \rho^* C_{p_3} D_{34}^* / k_3$ is an "inert" reference Lewis number based on the properties of the fuel-side inert at ambient conditions and is taken to be unity. The flame temperature rise, $\Delta T \equiv T_F - T_0$, is determined by combining Eqs. (7a) and (7b) with Eq. (5) to give

$$\Delta T_F = \frac{q \kappa_{01}}{C_{p_3}} Le_3 \times \frac{[(D_{1m}^*/D_{34}^*) F_1'(\hat{\eta})][G(+\infty) - G(\hat{\eta})][G(\hat{\eta}) - G(-\infty)]}{[F_1(+\infty) - F_1(\hat{\eta})][(k^*/k_3) G'(\hat{\eta})][G(+\infty) - G(-\infty)]} \qquad (8)$$

Results and Discussion

The effects of combined preferential energy and species transport on the normalized flame temperature rise indicated by this analysis are shown by the solid curves in Fig. 1. The reference value ΔT_{F_0} reflects the flame temperature rise of a flame with no preferential transport (i.e., $Le_1 \equiv Le_2 \equiv 1$) at a given equivalence ratio. The cases in Fig. 1 correspond to the diffusion of a highly diffusive fuel and a less mobile oxidizer into inerts with different thermal properties. The transport properties are taken to vary by a factor of two; such variations can be easily realized in common gases. Mass diffusivities far from the flame zone are identical for all cases ($D_{13}^*/D_{34}^* = D_{14}^*/D_{34}^* = 2$, $D_{23}^*/D_{34}^* = D_{24}^*/D_{34}^* = 1$); thermal transport varies in each case according to the properties of the inerts selected. For the diffusivities considered here, the case with preferential diffusion of mass only (case A, $C_{p4}/C_{p3} = k_4^*/k_3^* = 1$) exhibits a moderate effect on normalized flame temperature rise.[3-6] The addition of preferential thermal transport (cases B–E) results in a notable additional effect on the normalized flame temperature rise. When the more diffusive fuel is on the same side as the inert with the lower specific heat (case B, $C_{p4}/C_{p3} = 2$, $k_4^*/k_3^* = 1$) or higher thermal conductivity (case C, $C_{p4}/C_{p3} = 1$, $k_4^*/k_3^* = 0.5$), the flame temperature is higher than for the case with preferential mass diffusion only, and the normalized flame temperature rise exhibits a maximum near unity equivalence ratio. Maxima are not observed when the inerts are reversed (case D, $C_{p4}/C_{p3} = 0.5$, $k_4^*/k_3^* = 1$; case E, $C_{p4}/C_{p3} = 1$, $k_4^*/k_3^* = 2$), and the flame temperature rise is less than for the case of preferential mass diffusion alone. A change in the ratio of the ambient thermal conductivities (cases C and E) has a somewhat different impact on the normalized flame temperature rise than that produced by a change in inert specific heats (cases B and D). (This difference is not an artifact of the normalization of the temperature rise by the reference temperature ΔT_{F_0}; the temperature rise without normalization also shows a difference depending on whether the specific heat or thermal conductivity is varied.)

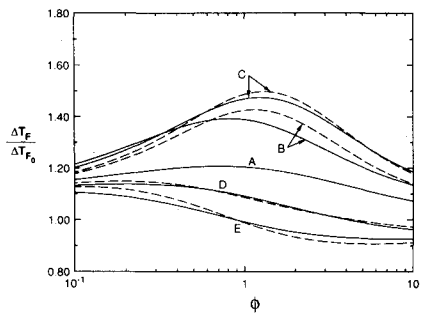

Fig. 1 Effects of combined preferential thermal and mass transport on normalized adiabatic flame temperature rise.

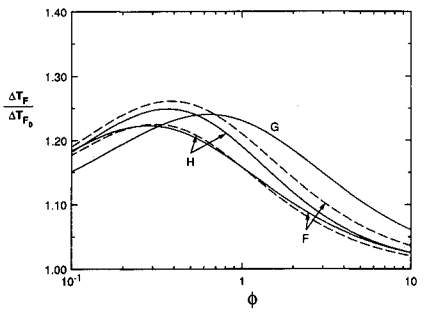

Fig. 2 Comparison of isolated effects of preferential thermal and mass transport on normalized adiabatic flame temperature rise.

Although this problem cannot be characterized in terms of the ambient values of the Lewis numbers alone, a reasonable approximation to the complete solution derived in this work can be obtained by taking Lewis numbers throughout the flowfield to be equal to the their values at the flame front. These results are indicated by the broken curves in Fig. 1. The full solution [Eq. (8)] and the calculation based on Lewis numbers at the flame front are in fairly close agreement. The discrepancies seen when the preferential thermal transport is due to differences in mixture specific heat capacity (cases B and D) are due in part to the diffusive transport of enthalpy resulting from the interdiffusion of inerts with difference heat capacities [cf., Eq. (3)].

A comparison of isolated effects of preferential mass diffusion and preferential thermal diffusion is made in Fig. 2. The cases F–H correspond, respectively, to separate variation in the mass diffusivities, specific heat capacities, and thermal conductivities for the same ambient reactant Lewis numbers. In each of the cases F–H, $D_{13}^*/D_{34}^* = D_{23}^*/D_{34}^* = 2$. The broken curves are generated by taking the mass diffusivity and thermal conductivity to scale linearly with inert mass fraction. In this case, all three curves have identical Lewis number profiles. In any event, these results indicate that, if preferential thermal and mass transport could be isolated, each preferential transport mechanism would give a different change in flame temperature rise for given Lewis numbers. The cases with preferential mass transport only (case F, $C_{p4}/C_{p3} = k_4^*/k_3^* = 1$, $D_{14}^*/D_{34}^* = D_{24}^*/D_{34}^* = 1$) and preferential thermal transport arising from differences in mixture thermal conductivity (case H, $C_{p4}/C_{p3} = 0.1$, $k_4^*/k_3^* = 2$, $D_{14}^*/D_{34}^* = D_{24}^*/D_{34}^* = 2$) are more similar than the case of preferential thermal transport arising from differences in mixture specific heat (case G, $C_{p4}/C_{p3} = 0.5$, $k_4^*/k_3^* = 1$, $D_{14}^*/D_{34}^* = D_{24}^*/D_{34}^* = 2$).

Summary

The effects of preferential thermal and preferential mass transport resulting from the interdiffusion of dissimilar inerts in a strained, laminar diffusion flame are examined. Preferential thermal transport results in notable changes in the adiabatic flame temperature rise compared with cases with the preferential diffusion of mass only. Even for a similar Lewis number profile, equivalent changes in mixture thermal conductivity and specific heat have a significantly different impact on the flame temperature rise. Substantial variations in reactant Lewis numbers due to the interdiffusion of dissimilar inerts preclude characterizing the effects of preferential thermal transport in terms of the ambient values. A formulation for flame temperature rise based on the local values of reactant Lewis numbers at the flame front provides reasonable agreement with the full analysis.

References

[1]Tsuji, H., "Counterflow Diffusion Flames," *Progress in Energy and Combustion Science,* Vol. 8, 1982, pp. 93-119.

[2]Peters, N., "Laminar Diffusion Flamelet Models in Non-Premixed Turbulent Combustion," *Progress in Energy and Combustion Science,* Vol. 10, 1984, pp. 319–339.

[3]Liñan, A., "Lewis Number Effects on the Structure and Extinction of Diffusion Flames Due to Strain," *The Role of Coherent Structures in Modelling Turbulence and Mixing,* edited by J. Jimenez, Vol. 136, Lecture Notes in Physics, Springer-Verlag, Berlin, Germany, 1981, p. 333.

[4]Law, C. K., and Chung, S. H., "Steady State Diffusion Flame Structure with Lewis Number Variations," *Combustion Science and Technology,* Vol. 29, Pts. 3-6, 1982, pp. 129–145.

[5]Chung, S. H., and Law, C. K., "Structure and Extinction of Convective Diffusion Flames with General Lewis Numbers," *Combustion and Flame,* Vol. 52, 1983, pp. 59–79.

[6]Seshadri, K., and Trevino, C., "The Influence of the Lewis Numbers of the Reactants on the Asymptotic Structure of Counterflow and Stagnant Diffusion Flames," *Combustion Science and Technology,* Vol. 64, Nos. 4–6, 1989, pp. 243–261.

[7]Hermanson, J. C., and Vranos, A., "Combined Effects of Preferential Thermal and Species Transport in a Strained, Laminar Diffusion Flame," *Combustion Science and Technology,* Vol. 75, Nos. 4–6, 1991, pp.339–345.

[8]Hermanson, J. C., and Vranos, A., "Preferential Thermal and Multicomponent Species Transport Effects in Strained Diffusion Flames with Fast Chemistry," United Technologies Research Center, UTRC Rept. 92-3, East Hartford, CT, April 1992.

[9]Curtiss, C. F., and Hirschfelder, J. O., "Transport Properties of Multicomponent Gas Mixtures," *The Journal of Chemical Physics,* Vol. 17, No. 6, 1949, pp. 550–555.

[10]Mason, E. A., and Saxena, S. C., "Approximate Formula for the Thermal Conductivity of Gas Mixtures," *Physics of Fluids,* Vol. 1, No. 5, 1958, pp. 361–369.

Comparison of Numerical Oblique Detonation Solutions with an Asymptotic Benchmark

Matthew J. Grismer* and Joseph M. Powers†
University of Notre Dame, Notre Dame, Indiana 46556

Introduction

THE design of aerospace vehicles of the present and future must take into account effects of compressibility, shock waves, multidimensionality, chemical reaction zones of various thicknesses, diffusive and radiative transport, and many other physical processes which are present in surrounding fluids. As it is often either prohibitively expensive or physically impossible to test aircraft under flight conditions and because the problems are typically analytically intractable, designers have come to rely on numerical methods to model these phenomena to predict flight performance. To have confidence in a numerical method, it is important to verify that it can reproduce known benchmark analytic solutions, available for simple model problems. A common benchmark is the inert oblique shock solution. Although valuable, this benchmark cannot quantify how well the numerical method predicts the effects of thick reaction zones.

This Note gives a new, more rigorous benchmarking procedure that is appropriate for numerical models of two-dimensional, high-speed reactive flows. The procedure is illustrated by comparing asymptotic and numerical solutions for oblique detonations, defined here as an attached oblique shock followed by an exothermic reaction with a thick reaction zone. The asymptotic solution, valid in the limit of high Mach number M_0, is given by Powers and Stewart,[1] who also give a review of the oblique detonation literature. For tractability, it was necessary in Ref. 1 to consider the fluid to be a calorically perfect ideal gas which undergoes a single-step irreversible exothermic reaction with Arrhenius kinetics in which the reactants and products have the same molecular weight. It was shown in Ref. 1 for such a fluid that an oblique detonation over a straight wedge consists of an attached shock with a downstream reaction and vorticity layer. The shock has maximum curvature at the wedge tip which relaxes to zero far from the wedge tip. Vorticity generated by the shock curvature is convected in a finite layer near the wedge surface. Heat release occurs in a finite layer parallel to the lead shock. Far from the shock and wedge surface the flow relaxes to an irrotational, equilibrium state.

The numerical solution was obtained with the RPLUS code,[2] in development at the NASA Lewis Research Center, using standard available features to simulate the flow. It is not our purpose to address issues which arise from the particular numerical method used in RPLUS. Rather, it is to show the utility of the asymptotic solution of Ref. 1 as a new benchmark. It should be possible in future studies to use this benchmark to critically assess the merits of differing numerical schemes for reacting flows.

As both the asymptotic and numerical solutions are approximations to a presumed exact solution, care must be exercised in determining the conditions under which the asymptotic solutions can be treated as a benchmark. For the second-order central differencing scheme of RPLUS, the numerical error is $\mathcal{O}(\Delta x^2)$ while the asymptotic error is $\mathcal{O}(\epsilon^2)$ (here $\epsilon = 1/M_0^2$). Thus for calculations on a fine fixed grid, one must employ high Mach numbers to insure that the asymptotic solution can be treated as a benchmark relative to the numerical solution. At lower Mach numbers the numerical solution gives a more accurate global estimate, but still contains local inaccuracies near shocks and boundaries. In such cases, the asymptotic solution retains value as a qualitative standard. For the comparisons of this Note, we study a Mach number range of $7.5 \leq M_0 \leq 20$. The asymptotic method, formally valid only when the ratio of chemical energy release to the kinetic energy of the flow is small, breaks down for lower Mach numbers and $\mathcal{O}(1)$ heat release.

We intend this Note to be of use to those developing codes to predict physical results. To this end, our procedure requires a compromise in model complexity in which only limited elements of real gas behavior at high Mach number are retained. Thus, our necessarily simple model ignores the temperature dependency of the specific heat, vibrational relaxation and dissociation effects, diffusive and radiative transport, turbulence, and the multicomponent, multireaction nature of real combustion processes. Nevertheless, it is a subset of models which include such effects. As such, the interested modeler can, as a first step, use the technique outlined here for the simple material. In so doing, the modeler can gain further confidence in the validity of his numerical method that will be used for the real gas, for which there is no benchmark reactive flow solution.

Model Equations

The dimensionless conservation and constitutive equations, nomenclature, and scaling are taken from Ref. 1. The scaling is such that all postshock quantities are $\mathcal{O}(1)$. With the asymptotic method, the leading-order solution is an inert oblique shock attached to a wedge inclined at angle θ; the effects of heat release are accounted for at $\mathcal{O}(\epsilon)$. The equations are

$$\frac{\partial}{\partial x}(\rho u) + \frac{\partial}{\partial y}(\rho v) = 0 \tag{1}$$

$$u\frac{\partial u}{\partial x} + v\frac{\partial u}{\partial y} + \frac{1}{\rho}\frac{\partial P}{\partial x} = 0 \tag{2}$$

Received Oct. 1, 1991; revision received June 2, 1992; accepted for publication June 5, 1992.

*Center for Applied Mathematics Graduate Fellow, Department of Aerospace and Mechanical Engineering. Student Member AIAA.

†Assistant Professor, Department of Aerospace and Mechanical Engineering. Member AIAA.